Performance Analysis for Uniform Linear Arrays Exploiting Two Coprime Frequencies

Muran Guo, Yimin D. Zhang, *Senior Member, IEEE,* and Tao Chen

***Abstract*—Sparse arrays can achieve a higher number of degrees of freedom (DOFs) compared with uniform linear array (ULA) counterparts. To further reduce the number of physical sensors while keeping a high number of DOFs, a direction of arrival (DOA) estimation algorithm by exploiting coprime frequencies base on a sparse ULA is recently proposed. However, the performance of such approach is not properly analyzed. In this letter, we analyze the Cramér-Rao bound (CRB) as the lower bound of the DOA estimation performance. The difference between the results presented in this letter and the recent CRB results on sparse arrays lies primarily in the additional phases occurred when utilizing different frequencies. It is shown in this letter that the phases affect the covariance matrix of the received data vector and, as a result, change the number of resolvable sources and alter the achieved CRB. We first demonstrate the effect of the additional phases with an example of two closely spaced sources, and the CRB for a sparse ULA exploiting two coprime frequencies is then derived. Numerical simulations are provided to validate the analyses.**

***Index Terms*—DOA estimation, Cramér-Rao bound, coprime frequencies, performance analysis.**

I. Introduction

To obtain higher degrees of freedom (DOFs) with a given number of sensors, sparse arrays, such as nested arrays [1] and coprime arrays [2], [3], have been proposed recently. Auto-correlation information is exploited in the direction of arrival (DOA) estimation based on sparse arrays. Generally, $\mathcal{O}(N^2)$ uncorrelated far-field narrowband sources can be estimated through $\mathcal{O}(N)$ sensors. To evaluate the performance of sparse arrays, the Cramér-Rao bound (CRB) for sparse arrays was derived in [4]–[6]. The offerings of coprime arrays have been experimentally validated in, e.g., [7]–[9].

Utilizing the fact that the array manifold matrix is related to the signal frequencies, a DOA estimation method based on a sparse uniform linear array (ULA) exploiting two or more coprime frequencies is proposed in [10], [11] to achieve a high number of degrees of freedom with much less sensors. By using two coprime frequencies, the number of physical sensors is approximately reduced to half as compared to the conventional coprime arrays. The coprime frequencies structure has gained considerable attention once proposed. For example, signals with coprime frequencies are exploited to interpolate the holes in the difference coarray of coprime arrays [12]. In this case, only a special scenario is considered and no phase difference between different frequency components are taken into account. Recently, DOA estimation using signals with coprime frequencies is examined in the context of high-order statistics [13]. Similar to [11], it mainly focuses on the achievable degrees of freedom, and no performance analysis is provided. A related work is to utilize coprime frequency signals to implement frequency diverse array for target localization [14].

In this letter, we focus on analyzing the performance of coprime frequencies structure, especially the effect of the phases difference between the signal components observed from different frequencies. Such signals indeed have unknown phase differences due to the frequency-dependent target reflectivity and different propagation phase delays. As a result, the CRB derived for conventional sparse arrays [6]–[8] cannot be readily applied to evaluate the performance of the array structure using coprime frequencies. To the best knowledge of the authors, the performance for ULA exploiting coprime frequencies has not been considered so far. In this letter, we first analyze the effect caused by additional phases in two closely spaced sources scenario and find that the angular resolution becomes better and better as the phase difference increases. Then, the CRB for ULA exploiting two coprime frequencies is derived and the corresponding performance is analyzed based on the CRB. An interesting result indicated by the CRB is that more sources can be resolved in presence of additional phases. Simulation results verify the analysis.

This letter is organized as follows. In Section II, we first introduce the system model and then briefly analyze the effect of the phase difference in two close source scenario. The CRB for ULA exploiting two coprime frequencies is derived in Section III. Simulation results are shown in Section IV to verify the analysis. Section V concludes this letter.

II. Preliminaries

A. System Model

Assume that an L-sensor ULA receives two continuous-wave (CW) signals whose carrier frequencies are associated

This work of M. Guo was supported by the China Scholarship Council (CSC) for his stay at the Temple University. The work of Y. D. Zhang was supported in part by the National Science Foundation (NSF) under grant AST-1547420. This work of T. Chen was supported by the National Natural Science Foundation of China (No. 61571146) and the Fundamental Research Funds for the Central Universities (HEUCFP201769). *(Corresponding author: Tao Chen.)*

M. Guo is with the College of Information and Communication Engineering, Harbin Engineering University, Harbin, 150001, China, and also with the Department of Electrical and Computer Engineering, Temple University, Philadelphia, PA 19122, USA (e-mail: guomuran@hrbeu.edu.cn).

Y. D. Zhang is with the Department of Electrical and Computer Engineering, Temple University, Philadelphia, PA 19122, USA (e-mail: ydzhang@temple.edu).

T. Chen is with the College of Information and Communication Engineering, Harbin Engineering University, Harbin, 150001, China (e-mail: chentao@hrbeu.edu.cn).

by a coprime relationship [11]. More specifically, the two frequencies f_1 and f_2 can be expressed as $f_k = M_k f_0$ with $k = 1, 2$, where M_1 and M_2 are a pair of coprime integers and f_0 is referred to as the base frequency. Equivalently, we can express the corresponding wavelength as $\lambda_k = \lambda_0/M_k$, where $\lambda_0 = c/f_0$ is the wavelength associated with the base frequency and $\lambda_k = c/f_k$. Denote $d_0 = \lambda_0/2$ as the unit interelement spacing. Assume Q far-field targets with DOAs $\theta_1, \theta_2, \cdots, \theta_Q$ impinge on the array, and let $\omega_q = \sin(\theta_q)$ with $q = 1, 2, \cdots, Q$. Then, the baseband model or the received returned signal vector associated with frequency f_k is expressed as [11]

$$\begin{aligned}\mathbf{x}^{(k)}(t) =& \sum_{q=1}^{Q} \rho_q^{(k)}(t)\mathbf{a}^{(k)}(\omega_q) + \mathbf{n}^{(k)}(t) \\ =& \mathbf{A}^{(k)}\mathbf{s}^{(k)}(t) + \mathbf{n}^{(k)}(t),\end{aligned} \tag{1}$$

for $t = 1, 2, \cdots, N$, where $\mathbf{s}^{(k)}(t) = [\rho_1^{(k)}(t), \cdots, \rho_Q^{(k)}(t)]$ and $\rho_q^{(k)}(t)$ is the complex envelop of the signal q at frequency f_k. We assume that $\rho_q^{(k)}(t)$ is uncorrelated for different targets. In addition, $\mathbf{A}^{(k)} = \left[\mathbf{a}^{(k)}(\omega_1), \cdots, \mathbf{a}^{(k)}(\omega_Q)\right]$ is the array manifold matrix, and $\mathbf{a}^{(k)}(\omega_q)$ is the steering vector of the qth target at frequency f_k and is expressed as

$$\begin{aligned}\mathbf{a}^{(k)}(\omega_q) &= \left[1, e^{j2\pi d_0\omega_q/\lambda_k}, \cdots, e^{j2\pi(L-1)d_0\omega_q/\lambda_k}\right]^T \\ &= \left[1, e^{j\pi M_k\omega_q}, \cdots, e^{j\pi(L-1)M_k\omega_q}\right]^T,\end{aligned} \tag{2}$$

where $(\cdot)^T$ denotes the transpose operator. Furthermore, $\mathbf{n}^{(k)}(t)$ is additive complex white Gaussian noise, independent from the target return signals, with mean zero and covariance matrix $p_{nk}\mathbf{I}_L$, i.e., $\mathbf{n}^{(k)}(t) \sim CN(\mathbf{0}, p_{nk}\mathbf{I}_L)$, where $\mathbf{I}_L$ is the $L \times L$ identity matrix.

For brevity, denote $\mathbf{s}^{(1)}(t)$ as $\mathbf{s}(t)$. Due to the different propagation phase delays and target reflectivity between the two frequencies, additional phases occur in the received signal of the second frequency with respect to difference targets [10]. Thus, $\mathbf{s}^{(2)}(t)$ can be expressed as $\mathbf{s}^{(2)}(t) = \mathbf{B}\mathbf{s}(t)$, where $\mathbf{B} = \text{diag}\left([e^{j\phi_1}, \cdots, e^{j\phi_Q}]\right)$ is the additional phase matrix, $j = \sqrt{-1}$, and diag$(\cdot)$ represents a diagonal matrix with the argument as its diagonal entries. Stacking the received return signals at both frequencies yields

$$\mathbf{x}(t) = \widetilde{\mathbf{A}}\mathbf{s}(t) + \mathbf{n}(t), \quad t = 1, 2, \cdots, N, \tag{3}$$

where $\mathbf{x}(t) = [(\mathbf{x}^{(1)}(t))^T, (\mathbf{x}^{(2)}(t))^T]^T$, $\widetilde{\mathbf{A}} = [(\mathbf{A}^{(1)})^T, (\mathbf{A}^{(2)}\mathbf{B})^T]^T = [\widetilde{\mathbf{a}}(\omega_1), \cdots, \widetilde{\mathbf{a}}(\omega_Q)]$, and $\mathbf{n}(t) = [(\mathbf{n}^{(1)}(t))^T, (\mathbf{n}^{(2)}(t))^T]^T$. $\widetilde{\mathbf{a}}(\omega_q)$ is the qth column of $\widetilde{\mathbf{A}}$ and is expressed as

$$\begin{aligned}\widetilde{\mathbf{a}}(\omega_q) = \Big[&1, e^{j\pi M_1\omega_q}, \cdots, e^{j\pi(L-1)M_1\omega_q}, e^{j\phi_q}, \\ &e^{j(\pi M_2\omega_q+\phi_q)}, \cdots, e^{j(\pi(L-1)M_2\omega_q+\phi_q)}\Big]^T.\end{aligned} \tag{4}$$

Thus, the covariance matrix of the combined data vector $\mathbf{x}(t)$ is given by

$$\mathbf{R}_{xx} = \widetilde{\mathbf{A}}\mathbf{R}_{ss}\widetilde{\mathbf{A}}^H + \mathbf{R}_{nn}, \tag{5}$$

where $\mathbf{R}_{ss} = \text{diag}([p_1, \cdots, p_Q])$ with p_q denoting the power of the qth returned signal, $\mathbf{R}_{nn} = \text{diag}([p_{n1}, p_{n2}]) \otimes \mathbf{I}_L$ with $\otimes$ denoting the Kronecker product operator, and $(\cdot)^H$ denotes the Hermitian operator.

B. Effects of Phase Difference

According to (4), an additional phase ϕ_q is introduced in the steering vector for the second frequency corresponding to the the qth target. In order to understand the effect of this phase difference, we first define the spatial correlation coefficient between two complex steering vectors $\mathbf{u}$ and $\mathbf{v}$ as

$$\gamma_{\mathbf{u},\mathbf{v}} = \frac{\mathbf{u}^H\mathbf{v}}{\|\mathbf{u}\|\|\mathbf{v}\|}. \tag{6}$$

Consider the scenario of two closely spaced targets with DOAs ω_1 and ω_2. Without loss of generality, let $\omega_1 < \omega_2$, and denote $\Delta\omega = \omega_2 - \omega_1$ and $\Delta\phi = \phi_2 - \phi_1$. Then, we obtain

$$\widetilde{\mathbf{a}}^H(\omega_1)\widetilde{\mathbf{a}}(\omega_2) = \sum_{i=1}^{L} e^{j\pi(i-1)M_1\Delta\omega} + e^{j\Delta\phi}\sum_{i=1}^{L} e^{j\pi(i-1)M_2\Delta\omega}. \tag{7}$$

By letting $x_1(i) = \pi(i-1)M_1\Delta\omega$ and $x_2(i) = \pi(i-1)M_2\Delta\omega$, (7) can be simplified as

$$\widetilde{\mathbf{a}}^H(\omega_1)\widetilde{\mathbf{a}}(\omega_2) = \sum_{i=1}^{L} e^{jx_1(i)} + e^{j\Delta\phi}\sum_{i=1}^{L} e^{jx_2(i)}. \tag{8}$$

To clearly demonstrate the effects of $\Delta\phi$, we consider a special case in which the two sources are from the same direction, i.e., $\Delta\omega = 0$. In this case, $x_1(i) = x_2(i) = 0$ always holds, and (8) becomes

$$\widetilde{\mathbf{a}}^H(\omega_1)\widetilde{\mathbf{a}}(\omega_2) = L(1 + e^{j\Delta\phi}). \tag{9}$$

The magnitude of the correlation coefficient between $\widetilde{\mathbf{a}}(\omega_1)$ and $\widetilde{\mathbf{a}}(\omega_1)$ is expressed as

$$\begin{aligned}\left|\gamma_{\widetilde{\mathbf{a}}(\omega_1),\widetilde{\mathbf{a}}(\omega_2)}\right| =& \frac{\left\|\widetilde{\mathbf{a}}^H(\omega_1)\widetilde{\mathbf{a}}(\omega_2)\right\|}{\|\widetilde{\mathbf{a}}(\omega_1)\|\,\|\widetilde{\mathbf{a}}(\omega_2)\|} \\ =& \frac{|1 + e^{j\Delta\phi}|}{2} = \left[\frac{1}{2}(1 + \cos\Delta\phi)\right]^{1/2}.\end{aligned} \tag{10}$$

It is well known that, under the conventional array processing scheme, two targets with identical DOAs yields a unit spatial correlation coefficient and cannot be resolved. From (10), however, we observe that $\left\|\gamma_{\widetilde{\mathbf{a}}(\omega_1),\widetilde{\mathbf{a}}(\omega_2)}\right\|$ varies with $\Delta\phi$. As $\Delta\phi$ increases from 0 to π, $\left\|\gamma_{\widetilde{\mathbf{a}}(\omega_1),\widetilde{\mathbf{a}}(\omega_2)}\right\|$ varies from 1 to 0. As a result, the angular resolution is improved. Thus, the existence of $\Delta\phi$ is likely to improve the angular resolution for closely spaced targets. This is an important feature which is desirable in applications that handle closely spaced targets.

III. Cramer-Rao Bound Results

Define $\mathbb{S} = \{0, M_1, \cdots, (L-1)M_1, 0, M_2, \cdots, (L-1)M_2\}$ as the equivalent arrays corresponding to the two frequencies. Note that location 0 appears twice as it is included in both arrays associated with the two frequencies. Let

$$\mathbb{D} = \{\mu - \nu | \mu, \nu \in \mathbb{S}\}. \tag{11}$$

We define the following real-valued parameter vector,

$$\boldsymbol{\alpha} = \begin{bmatrix} \boldsymbol{\Omega}^T & \boldsymbol{\rho}^T & \boldsymbol{\phi}^T & p_{n1} & p_{n2} \end{bmatrix}^T, \tag{12}$$

where $\boldsymbol{\Omega} = [\omega_1, \cdots, \omega_Q]^T$ and $\boldsymbol{\rho} = [p_1, \cdots, p_Q]^T$.

Under the previous assumptions and the Gaussian hypothesis, we can express the Fisher information matrix (FIM) as [4], [15]–[17]

$$\frac{1}{N}\text{FIM} = \left[\left(\mathbf{R}_{xx}^T \otimes \mathbf{R}_{xx} \right)^{-\frac{1}{2}} \frac{\partial \mathbf{r}_{xx}}{\partial \boldsymbol{\alpha}^T} \right]^H \left[\left(\mathbf{R}_{xx}^T \otimes \mathbf{R}_{xx} \right)^{-\frac{1}{2}} \frac{\partial \mathbf{r}_{xx}}{\partial \boldsymbol{\alpha}^T} \right]. \tag{13}$$

Because we are interested in the CRB of the DOAs, the parameter vector $\boldsymbol{\alpha}$ is divided as

$$\boldsymbol{\alpha} = \begin{bmatrix} \boldsymbol{\Omega}^T & | & \boldsymbol{\rho}^T & \boldsymbol{\phi}^T & p_{n1} & p_{n2} \end{bmatrix}^T. \tag{14}$$

Then, follow the derivation in [4], if FIM is invertible, the CRB for $\boldsymbol{\Omega}$ can be expressed as [18]

$$\text{CRB}(\boldsymbol{\Omega}) = \frac{1}{N} (\mathbf{G}^H \boldsymbol{\Pi}_{\boldsymbol{\Delta}}^{\perp} \mathbf{G})^{-1}, \tag{15}$$

where $\boldsymbol{\Pi}_{\boldsymbol{\Delta}}^{\perp} = \mathbf{I} - \boldsymbol{\Delta}(\boldsymbol{\Delta}^H \boldsymbol{\Delta})^{-1} \boldsymbol{\Delta}^H$. $\mathbf{G}$ and $\boldsymbol{\Delta}$ are defined as

$$\begin{aligned} \mathbf{G} &= \left(\mathbf{R}_{xx}^T \otimes \mathbf{R}_{xx} \right)^{-\frac{1}{2}} \left[\frac{\partial \mathbf{r}_{xx}}{\partial \omega_1}, \cdots, \frac{\partial \mathbf{r}_{xx}}{\partial \omega_Q} \right], \\ \boldsymbol{\Delta} &= \left(\mathbf{R}_{xx}^T \otimes \mathbf{R}_{xx} \right)^{-\frac{1}{2}} \\ &\quad \cdot \left[\frac{\partial \mathbf{r}_{xx}}{\partial p_1}, \cdots, \frac{\partial \mathbf{r}_{xx}}{\partial p_Q}, \frac{\partial \mathbf{r}_{xx}}{\partial \phi_1}, \cdots, \frac{\partial \mathbf{r}_{xx}}{\partial \phi_Q}, \frac{\partial \mathbf{r}_{xx}}{\partial p_{n1}}, \frac{\partial \mathbf{r}_{xx}}{\partial p_{n2}} \right]. \end{aligned} \tag{16}$$

Vectorizing the covariance matrix $\mathbf{R}_{xx}$ in (5) yields

$$\mathbf{r}_{xx} = \sum_{q=1}^{Q} p_q \widetilde{\mathbf{a}}^*(\omega_q) \otimes \widetilde{\mathbf{a}}(\omega_q) + \text{vec}\left(\mathbf{R}_{nn}\right), \tag{17}$$

since $\text{vec}\left(\mathbf{u}\mathbf{v}^T\right) = \mathbf{v} \otimes \mathbf{u}$ [19]. The term $\widetilde{\mathbf{a}}^*(\omega_q) \otimes \widetilde{\mathbf{a}}(\omega_q)$ can be further simplified as

$$\begin{aligned} &\widetilde{\mathbf{a}}^*(\omega_q) \otimes \widetilde{\mathbf{a}}(\omega_q) \\ &= \begin{bmatrix} \mathbf{a}^{(1)*}(\omega_q) \\ \mathbf{a}_2^{(2)*}(\omega_q) e^{-j\phi_q} \end{bmatrix} \otimes \begin{bmatrix} \mathbf{a}^{(1)}(\omega_q) \\ \mathbf{a}_2^{(2)}(\omega_q) e^{j\phi_q} \end{bmatrix} \\ &= \left\{ \begin{bmatrix} \mathbf{I}_L & \mathbf{0} \\ \mathbf{0} & \mathbf{I}_L e^{-j\phi_q} \end{bmatrix} \begin{bmatrix} \mathbf{a}^{(1)}(\omega_q) \\ \mathbf{a}_2^{(2)}(\omega_q) \end{bmatrix}^* \right\} \\ &\quad \otimes \left\{ \begin{bmatrix} \mathbf{I}_L & \mathbf{0} \\ \mathbf{0} & \mathbf{I}_L e^{j\phi_q} \end{bmatrix} \begin{bmatrix} \mathbf{a}^{(1)}(\omega_q) \\ \mathbf{a}_2^{(2)}(\omega_q) \end{bmatrix} \right\} \\ &= \left\{ \begin{bmatrix} \mathbf{I}_L & \mathbf{0} \\ \mathbf{0} & \mathbf{I}_L e^{-j\phi_q} \end{bmatrix} \otimes \begin{bmatrix} \mathbf{I}_L & \mathbf{0} \\ \mathbf{0} & \mathbf{I}_L e^{j\phi_q} \end{bmatrix} \right\} \\ &\quad \cdot \left\{ \begin{bmatrix} \mathbf{a}^{(1)}(\omega_q) \\ \mathbf{a}_2^{(2)}(\omega_q) \end{bmatrix}^* \otimes \begin{bmatrix} \mathbf{a}^{(1)}(\omega_q) \\ \mathbf{a}_2^{(2)}(\omega_q) \end{bmatrix} \right\} \\ &= \mathbf{F}_q \mathbf{J} \mathbf{a}_{\mathbb{D}}(\omega_q), \end{aligned} \tag{18}$$

where the property $(\mathbf{AB}) \otimes (\mathbf{CD}) = (\mathbf{A} \otimes \mathbf{C})(\mathbf{B} \otimes \mathbf{D})$ is utilized [19]. In the above expression, $\mathbf{a}_{\mathbb{D}}(\omega_q)$ is the steering vector of the qth target based on the coarray with locations $\{\bar{d} d_0 | \bar{d} \in \mathbb{D}\}$ and $\mathbf{J}$ is the binary matrix [4] such that $[(\mathbf{a}^{(1)}(\omega_q))^T \quad (\mathbf{a}_2^{(2)}(\omega_q))^T]^H \otimes [(\mathbf{a}^{(1)}(\omega_q))^T \quad (\mathbf{a}_2^{(2)}(\omega_q))^T]^T = \mathbf{J}\mathbf{a}_{\mathbb{D}}(\omega_q)$. $\mathbf{F}_q$ only depends on the phase ϕ_q and is expressed as

$$\mathbf{F}_q = \begin{bmatrix} \mathbf{I}_L & \mathbf{0} \\ \mathbf{0} & \mathbf{I}_L e^{-j\phi_q} \end{bmatrix} \otimes \begin{bmatrix} \mathbf{I}_L & \mathbf{0} \\ \mathbf{0} & \mathbf{I}_L e^{j\phi_q} \end{bmatrix}. \tag{19}$$

By substituting (18) into (17), the vectorized covariance matrix $\mathbf{r}_{xx}$ is simplified as

$$\mathbf{r}_{xx} = \sum_{q=1}^{Q} p_q \mathbf{F}_q \mathbf{J} \mathbf{a}_{\mathbb{D}}(\omega_q) + \text{vec}\left(\mathbf{R}_{nn}\right). \tag{20}$$

To obtain the CRB for two coprime frequencies, we then take the derivative of $\mathbf{r}_{xx}$ with respect to $\boldsymbol{\alpha}$. By utilizing (20) we obtain

$$\begin{aligned} \frac{\partial \mathbf{r}_{xx}}{\partial \omega_q} &= p_q \mathbf{F}_q \mathbf{J} \frac{\partial \mathbf{a}_{\mathbb{D}}(\omega_q)}{\partial \omega_q} \\ &= j\pi p_q \mathbf{F}_q \mathbf{J} \text{diag}(\mathbb{D}) \mathbf{a}_{\mathbb{D}}(\omega_q). \end{aligned} \tag{21}$$

Similarly, the partial of $\mathbf{r}_{xx}$ with respect to the rest of the parameter vector can be expressed as

$$\frac{\partial \mathbf{r}_{xx}}{\partial p_q} = \mathbf{F}_q \mathbf{J} \mathbf{a}_{\mathbb{D}}(\omega_q), \tag{22}$$

$$\begin{aligned} \frac{\partial \mathbf{r}_{xx}}{\partial \phi_q} &= p_q \frac{\partial \mathbf{F}_q}{\partial \phi_q} \mathbf{J} \mathbf{a}_{\mathbb{D}}(\omega_q) \\ &= p_q \frac{\partial \left\{ \begin{bmatrix} \mathbf{I}_L & \mathbf{0} \\ \mathbf{0} & \mathbf{I}_L e^{-j\phi_q} \end{bmatrix} \otimes \begin{bmatrix} \mathbf{I}_L & \mathbf{0} \\ \mathbf{0} & \mathbf{I}_L e^{j\phi_q} \end{bmatrix} \right\}}{\partial \phi_q} \mathbf{J} \mathbf{a}_{\mathbb{D}}(\omega_q) \\ &= p_q \left\{ \begin{bmatrix} \mathbf{0} & \mathbf{0} \\ \mathbf{0} & -j\mathbf{I}_L e^{-j\phi_q} \end{bmatrix} \otimes \begin{bmatrix} \mathbf{I}_L & \mathbf{0} \\ \mathbf{0} & \mathbf{I}_L e^{j\phi_q} \end{bmatrix} \right. \\ &\quad \left. + \begin{bmatrix} \mathbf{I}_L & \mathbf{0} \\ \mathbf{0} & \mathbf{I}_L e^{-j\phi_q} \end{bmatrix} \otimes \begin{bmatrix} \mathbf{0} & \mathbf{0} \\ \mathbf{0} & j\mathbf{I}_L e^{j\phi_q} \end{bmatrix} \right\} \mathbf{J} \mathbf{a}_{\mathbb{D}}(\omega_q) \\ &= p_q \mathbf{F}'_q \mathbf{J} \mathbf{a}_{\mathbb{D}}(\omega_q), \end{aligned} \tag{23}$$

$$\frac{\partial \mathbf{r}_{xx}}{\partial p_{n1}} = \text{vec}\left(\begin{bmatrix} \mathbf{I}_L & \mathbf{0} \\ \mathbf{0} & \mathbf{0} \end{bmatrix} \right), \quad \frac{\partial \mathbf{r}_{xx}}{\partial p_{n2}} = \text{vec}\left(\begin{bmatrix} \mathbf{0} & \mathbf{0} \\ \mathbf{0} & \mathbf{I}_L \end{bmatrix} \right). \tag{24}$$

In (23), $\text{d}(\mathbf{X} \otimes \mathbf{Y}) = (\text{d}\mathbf{X}) \otimes \mathbf{Y} + \mathbf{X} \otimes (\text{d}\mathbf{Y})$ is utilized [19]. Substituting (21)–(24) into (16) and (15) will lead to the CRB for ULA exploiting two coprime frequencies.

IV. Simulation Results

In this section, we first verify the effects of phase difference in the case of two closely spaced sources. The CRB versus the number of snapshots and SNR are then examined in terms of the empirical root mean square error (RMSE). Finally, we investigate the CRB versus the number of targets. The RMSE is defined as

$$\text{RMSE} = \left[\frac{1}{IQ} \sum_{i=1}^{I} \sum_{q=1}^{Q} (\hat{\theta}_q^{(i)} - \theta_q^{(i)})^2 \right]^{1/2}. \tag{25}$$

where $\hat{\theta}_q$ is the estimated DOA of the qth target.

Throughout this section, we consider a ULA with 4 sensors and use two coprime frequencies with $M_1 = 3$ and $M_2 = 4$. We assume the powers of the returned signals to be identical.

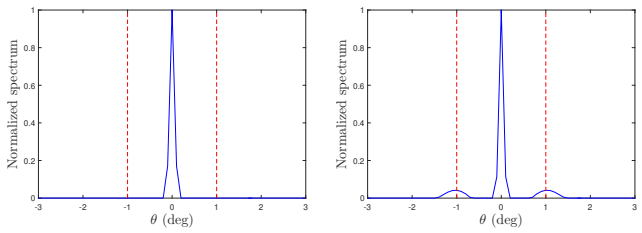

(a) $\Delta\phi = 0.4\pi$ (b) $\Delta\phi = 0.5\pi$

(c) $\Delta\phi = 0.6\pi$ (d) $\Delta\phi = 0.7\pi$

Fig. 1. The spatial spectra of two close sources with different phases.

In addition, the noise powers p_{n1} and p_{n2} are assumed to be the same. Furthermore, the phase of each source with respect to the second frequency is set as $2(q-1)\pi/Q$ with $q = 1, 2, \cdots, Q$. The group LASSO method is used for the estimation of the DOAs [10].

A. Effects of Phase Difference in the Case of Two Closely Spaced Targets

In Section II.B, we have shown that the identifiability can be improved for two closely spaced targets as the the phase difference between the two frequency components varies from 0 to π. To verify this claim, consider two targets with DOAs of $-1°$ and $1°$. To clearly understand the effect of the phase difference, we consider a noise-free scenario with 200,000 snapshots. Four different phase difference values, i.e., $\Delta\phi = 0.4\pi, 0.5\pi, 0.6\pi$ and 0.7π, are considered, and the results are shown in Fig. 1. It is observed that the two close sources become more resolvable as $\Delta\phi$ increases, which is consistent to the analysis in Section II.B.

B. Comparison of CRB and Empirical RMSE

Next, we examine the CRB of the two coprime frequency case with respect to the number of snapshots and the input SNR. 8 targets uniformly distributed between $-60°$ and $60°$ are considered here. The simulation results are given in Fig. 2. A gap is observed between the CRB and the empirical RMSE. Moreover, the decreasing ratio of empirical RMSE is smaller than that of CRB in Figure 2(a). One important reason that leads to this phenomenon is the DOAs of targets are not exactly lie on the grid of group LASSO.

C. CRB versus the Number of Targets

As analyzed in the previous sections, if the phase differences are zero, the two coprime frequency model is equivalent to a corresponding coprime array structure with a pair of coprime integers equaling M_1 and M_2. Note that different to the conventional coprime arrays where we assume different numbers of sensors in the two subarrays, the numbers of sensors in the underlying array structure are identical.

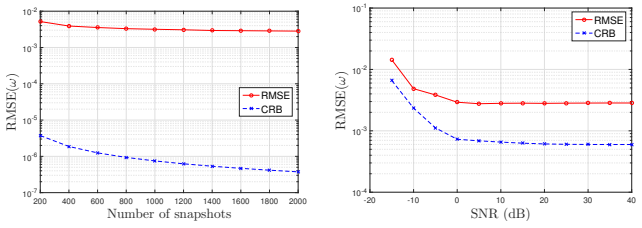

(a) CRB vs. the number of snapshots (b) CRB vs. SNR

Fig. 2. CRB for two coprime frequencies. (a) versus the number of snapshots (SNR=20 dB); (b) versus SNR (2,000 snapshots).

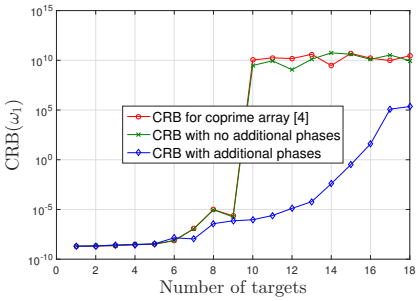

Fig. 3. CRB versus the number of targets with 20 dB SNR and 2000 snapshots.

Let the target DOAs uniformly distribute between $-60°$ and $60°$ for each index, and use 20 dB SNR and 2,000 snapshots. Fig. 3 shows an interesting result that more targets can be resolved by using two signals coprime frequencies in the presence of the phase differences. To verify this result, we also plot the spatial spectrum results in Fig. 4. In Fig. 4(a), 10 targets are considered and all the phase differences are set to zeros. As a result, the targets cannot be resolved correctly as indicated by the CRB. In contrast, 12 targets are considered in Fig. 4(b) in presence of the phase differences. Despite the more targets, the 12 targets are accurately resolved.

V. Conclusion

In this letter, we analyzed the DOA estimation performance for a sparse ULA exploiting two coprime frequencies. The effect induced by the phase difference in the two frequency signals generally improves the angular resolution of closely spaced targets. We then derived the corresponding CRB, and reveal that the additional phase difference can increase the number of resolvable targets. Finally, simulations results verified the theoretical analyses.

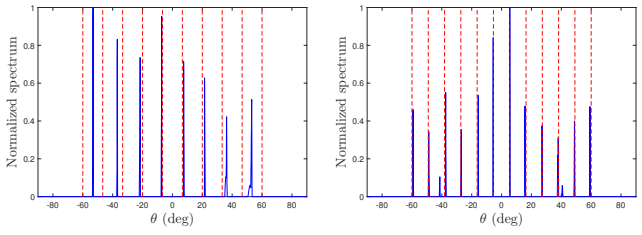

(a) (b)

Fig. 4. Spatial spectra with and without phase differences. (a) 10-target case with no phase differences. (b) 12-target case with random phase differences.

REFERENCES

[1] P. Pal and P. P. Vaidyanathan, "Nested arrays: A novel approach to array processing with enhanced degrees of freedom," *IEEE Trans. Signal Process.*, vol. 58, no. 8, pp. 4167–4181, Aug. 2010.

[2] P. P. Vaidyanathan and P. Pal, "Sparse sensing with co-prime samplers and arrays," *IEEE Trans. Signal Process.*, vol. 59, no. 2, pp. 573–586, Feb. 2011.

[3] S. Qin, Y. D. Zhang, and M. G. Amin, "Generalized coprime array configurations for direction-of-arrival estimation," *IEEE Trans. Signal Process.*, vol. 63, no. 6, pp. 1377–1390, Mar. 2015.

[4] C.-L. Liu and P. P. Vaidyanathan, "Cramér-Rao bounds for coprime and other sparse arrays, which find more sources than sensors," *Digital Signal Process.*, vol. 61, pp. 43–61, Feb. 2017.

[5] A. Koochakzadeh and P. Pal, "Cramér-Rao bounds for underdetermined source localization," *IEEE Signal Process. Lett.*, vol. 23, no. 7, pp. 919–923, Jul. 2016.

[6] M. Wang and A. Nehorai, "Coarrays, MUSIC, and the Cramér-Rao bound," *IEEE Trans. Signal Process.*, vol. 65, no. 4, pp. 933–946, Feb. 2017.

[7] N. Xiang, D. Bush, and J. Summers, "Experimental validation of a coprime linear microphone array for high-resolution direction-of-arrival measurements," *J. Acoust. Soc. Am.*, vol. 137, no. 4, pp. EL261–EL266, Feb. 2015.

[8] D. Bush and N. Xiang, "Broadband implementation of coprime linear microphone arrays for direction of arrival estimation," *J. Acoust. Soc. Am.*, vol. 138, no. 1, pp. 447-456, Jun. 2015.

[9] Q. Shen, W. Liu, W. Cui, S. Wu, Y. D. Zhang, and M. G. Amin, "Low-Complexity Direction-of-Arrival Estimation Based on Wideband Co-Prime Arrays," *IEEE/ACM Trans. Audio, Speech, Language Process.*, vol. 23, no. 9, pp. 1445-1456, Sep. 2015.

[10] Y. D. Zhang, M. G. Amin, F. Ahmad, and B. Himed, "DOA estimation using a sparse uniform linear array with two CW signals of co-prime frequencies," in *Proc. IEEE Int. Workshop Comput. Adv. Multi-Sensor Adapt. Process.*, Saint Martin, pp. 404–407, Dec. 2013.

[11] S. Qin, Y. D. Zhang, M. G. Amin, and B. Himed, "DOA estimation exploiting a uniform linear array with multiple co-prime frequencies," *Signal Process.*, vol. 130, pp. 37–46, Jan. 2017.

[12] E. BouDaher, Y. Jia, F. Ahmad, and M. G. Amin, "Multi-frequency co-prime arrays for high-resolution direction-of-arrival estimation," *IEEE Trans. Signal Process.*, vol. 63, no. 14, pp. 3797–3808, Jul. 2015.

[13] A. Ahmed, Y. D. Zhang, and B. Himed, "Cumulant-based direction-of-arrival estimation using multiple co-prime frequencies, in *Proc. Asilomar Conf. Signals, Systems, and Computers*, Pacific Grove, CA, Nov. 2017.

[14] S. Qin, Y. D. Zhang, M. G. Amin, and F. Gini, "Frequency diverse coprime arrays with coprime frequency offsets for multitarget localization," *IEEE J. Sel. Top. Signal Process.*, vol. 11, no. 2, pp. 321–335, Mar. 2017.

[15] P. Stocia and A. Nehorai, "MUSIC, maximum likelihood, and Cramer-Rao bound," *IEEE Trans. Acoust. Speech Signal Process.*, vol. 37, no. 5, pp. 720-741, May 1989.

[16] P. Stocia and R. L. Moses, *Introduction to Spectral Analysis*. Prentice-Hall, 1997.

[17] A. Weiss and B. Friedlander, "On the Cramer-Rao bound for direction finding of correlated signals," *IEEE Trans. Signal Process.*, vol. 41, no. 1, pp. 495-499, Jan. 1993.

[18] P. Stocia, E. G. Larsson, and A. B. Gershman, "The stochastic CRB for array processing: A textbook derivation," *IEEE Signal Process. Lett.*, vol. 8, no. 5, pp. 148–150, May 2001.

[19] G. H. Golub and C. F. Van Loan, *Matrix Computations, Third Edition*. Johns Hopkins Univ. Press, 1996.